



Pergamon

Structure of *Plasmodium vivax* Dihydrofolate Reductase Determined by Homology Modeling and Molecular Dynamics Refinement

Giulio Rastelli,* Sara Pacchioni and Marco Daniele Parenti

Dipartimento di Scienze Farmaceutiche, Università di Modena e Reggio Emilia. Via Campi 183, 41100 Modena, Italy

Received 19 March 2003; revised 11 June 2003; accepted 24 June 2003

Abstract—The structure of *Plasmodium vivax* dihydrofolate reductase (PvDHFR), a potentially important target for antimalarial chemotherapy, was determined by means of homology modeling and molecular dynamics refinement. The structure proved to be consistent with DHFRs of known crystal structure. The comparison of the complexes of the antifolate inhibitor pyrimethamine bound at the active sites of PvDHFR and PfDHFR, the related enzyme from *Plasmodium falciparum*, prospected the possibility of using structure-based drug design to develop inhibitors that are effective against both malarial enzymes. This study constitutes a first step toward understanding of the antifolate-PvDHFR molecular interactions and possible rationalization of resistance in *vivax* malaria.

© 2003 Elsevier Ltd. All rights reserved.

While *Plasmodium falciparum* dihydrofolate reductase-thymidylate synthase (PfDHFR-TS) has been extensively studied as a target to combat malaria,¹ *Plasmodium vivax* DHFR-TS (PvDHFR-TS) has received renewed attention only in the last few years. Firstly, there are increasing evidences of chloroquine resistance in *vivax* malaria,^{2–4} pressing the need for development of other families of antimalarials. Secondly, common occurrence of mixed infections of *P. vivax* and *P. falciparum* malaria might be appropriately dealt with by new antifolates which are effective against both types of parasites. Thirdly, but not lastly, both parasites have developed widespread resistance to commonly used antifolates, and understanding the structural bases of resistance is clearly a key step to combat malaria.

We previously reported models of *P. falciparum* DHFR enzyme based on the homology of the DHFR sequences.⁵ These models (wild type and selected antifolate resistant mutants) were exploited to study the molecular interactions of antifolate inhibitors such as Pyrimethamine, Cycloguanil and WR99210 with the enzyme binding site, in order to highlight structural

bases of antifolate resistance and to provide rational approaches for designing non-resistant inhibitors.^{5,6}

Here, we extend our studies to *P. vivax* DHFR (PvDHFR) by determining a model structure for this enzyme. To our knowledge, this is the first study that addresses such objective.

The structure of PvDHFR was obtained from homology modeling simulations. The sequence of PvDHFR was aligned with the DHFR sequences of which the crystal structures are known; these include *Escherichia coli*, *Lactobacillus casei*, human, chicken liver and *Pneumocystis carinii*. The sequence of the related PfDHFR was also included as a reference. The alignment reported in Figure 1 was made using ClustalW,⁷ and then manually refined to reflect the structurally conserved regions of the available crystal structures. This alignment is similar to that previously obtained for PfDHFR⁵: both PvDHFR and PfDHFR have two long insertions in their sequences (inserts 1 and 2 in Fig. 1) that do not have correspondence to other DHFRs of known structures. Therefore, in our previous model of PfDHFR they were modeled as loops. However, the prediction of secondary structure of both inserts using PHDsec⁸ made at the PredictProtein server of EMBL⁹ clearly suggests that part of insert 2 (residues 70–82) has very high probability of being in α -helical conformation.

*Corresponding author. Tel.: +39-0592-055145; fax: +39-0592-055131; e-mail: rastelli.giulio@unimo.it

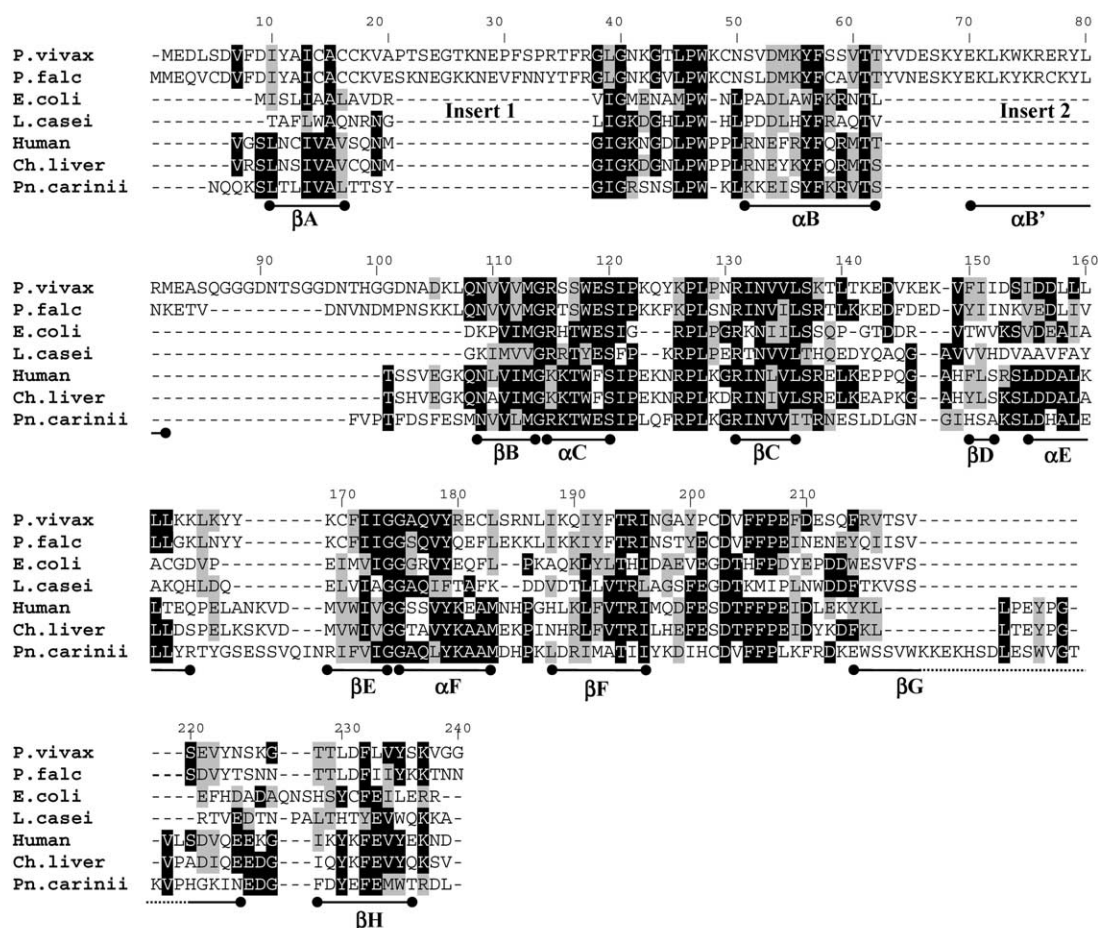


Figure 1. Alignment of the amino acid sequences of dihydrofolate reductase of *Plasmodium vivax*, *Plasmodium falciparum*, *Escherichia coli*, *Lactobacillus casei*, human, chicken liver and *Pneumocystis carinii*. The secondary structure is indicated as α and β . The two long insertions unique to PvDHFR and PfDHFR are shown (insertions 1 and 2). The newly identified α -helix is $\alpha B'$.

For this reason, a α -helix at residues 70–82, here termed $\alpha B'$ (Fig. 1), was explicitly requested when constructing the homology model of PvDHFR, which was made using Modeller v6.2.¹⁰ A detailed description of the procedure used to derive the homology model can be found in ref 5. Briefly, 10 models were generated and inspected. Of these, four had high modeler objective functions and were discarded. The remaining six models, with similar objective functions, were closely superimposable in the conserved regions but, as expected, showed remarkable variations in the two inserts. Notwithstanding, since five of these had $\alpha B'$ interacting with αB , albeit in different orientations, the model with the best objective function was saved for further refinement and validation. The model, which included the cofactor NADPH, was iteratively refined with molecular dynamics (MD) simulations using AMBER7.¹¹ Refinement included only the less conserved and non-structured regions first, which are the regions less accurately predicted by homology modeling. At this end, these residues were energy-minimized and subjected to 2ns MD at 300 K with distance-dependent dielectric constant to simulate the presence of water. During MD, insertion 1 and part of insertion 2 (residues 88–103) appeared to be fairly flexible. On the contrary, a stable folding could be detected for the beginning of insertion 2 (residues 63–69) and the following $\alpha B'$ helix (residues

70–82). Sequence alignment of PvDHFR and PfDHFR showed that residues 63–82 are highly conserved between the two species, while residues 83–105 of PvDHFR are characterized by an additional tandem repeat sequence GGDN that is absent in PfDHFR.¹² The high sequence similarity at the beginning of insert 2 suggests that helix $\alpha B'$ is likely present in PfDHFR as well, and supports the present finding that region 63–82 adopts a well defined fold. Refinement was then continued with a periodic box of 6631 water molecules and using PME for treating long-range electrostatics. In these new conditions, MD at 300 K was run for over 400 ps, with restraints on the conserved regions applied first and then gradually removed. Finally, the anti-malarial compound pyrimethamine (Pyr) was docked in the active site as previously proposed,⁵ and the ternary complex was energy-minimized.

The quality of the refined PvDHFR-NADPH-Pyr structure thus obtained was checked with PROCHECK¹³ and ProsaII.¹⁴ The structure satisfied the tests; in the Ramachandran plot, 73.1% of the residues were in the most favored regions, 23.1% in additional allowed regions, 1.9% in generously allowed regions, and 1.9% in disallowed regions (S184, K48, K163 and L165). ProsaII confirmed that a reasonable model was obtained, whose Z-score of -7.3 compares with

the averaged Z-score of -10.8 ± 1 for the five DHFR templates used. The RMS deviation between the PvDHFR structure and the DHFR crystal structures used as templates were computed for the backbone atoms (C, N, O, CA) of the more conserved and structured regions (Fig. 1). The RMS deviations from the templates are significantly low, being 0.77 Å with *E. coli*, 1.04 Å with *L. casei*, 1.11 Å with human, 1.07 Å with chicken liver, and 1.07 Å with *P. carinii* (PDB entry codes 1drh, 3dfr, 1dfr, 8dfr, 1dyr, respectively).

The PvDHFR refined structure is shown in Figure 2. The overall folding is very similar to that previously reported for other DHFRs.⁵ An eight-stranded β -sheet (β A– β H) consisting of seven parallel strands and a carboxy-terminal antiparallel strand composes the core of the protein, and four α -helices (α B, α C, α E and α F) are packed against the β -sheet core with an additional short α -helix at residues 123–125 also found in human and chicken liver DHFRs. Unlike invertebrate DHFRs, but similarly to vertebrate DHFRs,^{15,16} β G is not continuous but consists of two consecutive strands denoted G1, residues 214–218, and G2, residues 223–224. Compared to invertebrate DHFRs, the insertion of an additional aminoacid (S220) in PvDHFR (Fig. 1) could be responsible for the disruption of the β G-sheet hydrogen bonding. The two-turn α -helix α E', observed only in vertebrate DHFRs and located between α E and β E,^{15,16} is not predicted in the present structure. The cofactor NADPH is bound to PvDHFR in an extended conformation similar to that previously reported for other DHFRs, with nearly all the protein–cofactor interactions being conserved.

The newly predicted helix α B' mainly contacts the beginning of insertion 2 (residues 63–69) and the α B helix (Fig. 2); in agreement with the highly polar nature of this insertion, a number of hydrogen bonds and salt links are formed. While this study was reviewed, the crystal structure of the related dimeric PfDHFR-TS enzyme was reported.¹⁷ While the crystal structure revealed that insert 2 had α -helical character at residues

67–81, in agreement with our prediction, the α B' helix was located at the dimer interface. A different orientation of α B' is not surprising, given the lack of homology with the templates in this region and the fact that only the DHFR domain could be modeled in this study. PvDHFR-TS, in fact, exists as a dimer of identical subunits, with the DHFR domain linked to the TS domain by a long (100 residues) junction region which is not homologous to other sequences of known structure and for which no clear prediction of secondary structure could be obtained.^{12,18} Therefore, the contribution of the TS domain and of the other monomer could not be taken into account. However, we point out that α B' is at least 20 Å away from the active site, and it does not appear to alter the conformation of the most important part of the structure. Remarkably, the PvDHFR model compares well with the DHFR domain of the crystal structure of PfDHFR (with an RMS deviation of the more conserved backbone atoms of 1.1 Å), and the active sites are closely superimposable.

The structure of the antifolate Pyr bound at the active site of PvDHFR is reported in Figure 3 (upper). The 1-NH (protonated form) and the 2-NH₂ of Pyr form bidentate hydrogen bonds with D53, and the 4-NH₂ forms hydrogen bonds with the I13 and I173 backbone carbonyls. The 5-chlorophenyl ring stacks against F57

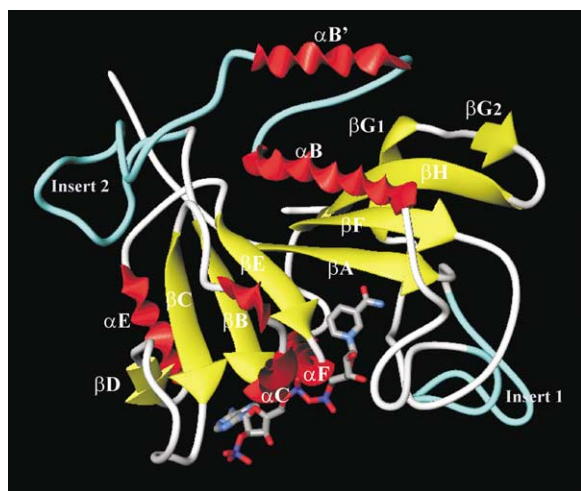


Figure 2. Homology model of PcDHFR. β sheets are colored in yellow, α helices are colored in red. Insertions 1 and 2 are colored in cyan. The cofactor NADPH is shown in stick.

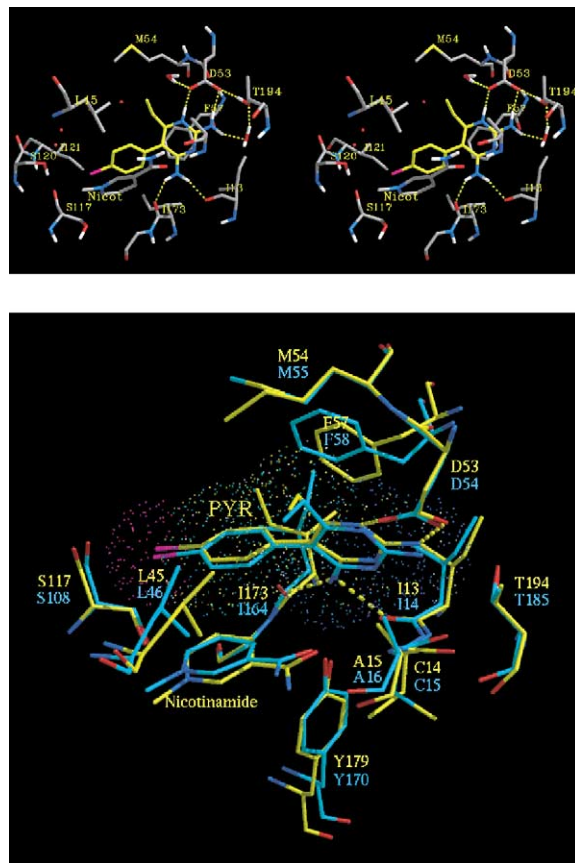


Figure 3. Upper: stereoview showing Pyr bound at the active site of PvDHFR. For clarity, only polar hydrogens are shown; lower: superimposition of the complexes of Pyr with PvDHFR (yellow) and PfDHFR (cyan).

and the nicotinamide ring of the cofactor. The chlorine atom approaches S117. Interestingly, these interactions are in all similar to those established with the PfDHFR enzyme.⁵

The superimposition between the present structure and the PfDHFR structure with Pyr bound⁵ (Fig. 3, lower) shows that the active site architecture is significantly similar between the two related enzymes, with all the residues contacting the antifolate (D53, A15, I173, I13, S117, F57, L45, T194, Y179 and M54) being conserved in the sequences and superimposed in the structures. Therefore, the present structure indeed prospects the possibility of using structure-based design to develop inhibitors that are effective against both PvDHFR and PfDHFR.

In conclusion, the present results constitute the first attempt to derive a model structure of the PvDHFR enzyme, and will be used to investigate enzyme-antifolate interactions with the wild type and resistant mutant enzymes.¹⁹

Acknowledgements

This work was supported by a grant from the European Union (INCO-DEV No. ICA4-CT-2001-10077).

References and Notes

1. Sirawaraporn, W. *Drug Resist. Update* **1998**, *1*, 397.
2. Schuurkamp, G. J.; Spiener, P. E.; Karen, R. K.; Bulungol, P. K. *Trans R. Soc. Trop. Med. Hyg.* **1989**, *83*, 607.
3. Schwartz, I. K.; Lackritz, E. M.; Patchen, L. C. *New Engl. J. Med.* **1991**, *324*, 927.
4. Garg, M.; Gopinathan, N.; Bodhe, P.; Kshirsagar, N. A. *Trans R. Soc. Trop. Med. Hyg.* **1995**, *89*, 656.
5. Rastelli, G.; Sirawaraporn, W.; Sompornpisut, P.; Vilaivan, T.; Kamchonwongpaisan, S.; Quarrel, R.; Lowe, G.; Thebtaranonth, Y.; Yuthavong, Y. *Bioorg. Med. Chem.* **2000**, *8*, 1117.
6. Yuthavong, Y.; Vilaivan, T.; Chareonsethakul, N.; Kamchonwongpaisan, S.; Sirawaraporn, W.; Quarrel, R.; Lowe, G. *J. Med. Chem.* **2000**, *43*, 2738.
7. Thompson, J. D.; Higgins, D. G.; Gibson, T. J. *Nucleic Acids Res.* **1994**, *22*, 4673.
8. Rost, B.; Sander, C. *J. Mol. Biol.* **1993**, *232*, 584.
9. www.embl-heidelberg.de/predictprotein/predictprotein.html
10. Sali, A.; Blundell, T. L. *J. Mol. Biol.* **1993**, *234*, 779.
11. Case, D. A.; Pearlman, D. A.; Caldwell, J. W.; Cheatham, T. E.; Wang, J.; Ross, W. S.; Simmerling, C. L.; Darden, T. A.; Merz, K. M.; Stanton, R. V.; Cheng, A. L.; Vincent, J. J.; Crowley, M.; Tsui, V.; Gohlke, H.; Radmer, R. J.; Duan, Y.; Pitera, J.; Massova, I.; Seibel, G. L.; Singh, U. C.; Weiner, P. K.; Kollman, P. A. AMBER 7; University of California: San Francisco, 2002.
12. de Pecoulas, P. E.; Basco, L. K.; Tahar, R.; Ouatas, T.; Mazabraud, A. *Gene* **1998**, *211*, 177.
13. Laskowski, R. A.; McArthur, M. W.; Moss, D. S.; Thornton, J. M. *J. Appl. Cryst.* **1993**, *26*, 283.
14. Sippl, M. J. *Proteins* **1993**, *17*, 355.
15. Davies, J. F., II; Delcamp, T. J.; Prendergast, N. J.; Ashford, V. A.; Freisheim, J. H.; Kraut, J. *Biochemistry* **1990**, *29*, 9467.
16. McTigue, M. A.; Davies, J. F., II; Kaufman, B. T.; Kraut, J. *Biochemistry* **1992**, *31*, 7264.
17. Yuvaniyama, J.; Chitnumsub, P.; Kamchonwongpaisan, S.; Vanichtanankul, J.; Sirawaraporn, W.; Taylor, P.; Walkinshaw, M. D.; Yuthavong, Y. *Nat. Struct. Biol.* **2003**, *10*, 357.
18. Bzik, D. J.; Li, W. B.; Horii, T.; Inselburg, J. *Proc. Natl. Acad. Sci. U.S.A.* **1987**, *84*, 8360.
19. The structure can be downloaded at: <http://far01.unimo.it/gruppi/rastelli/>